Weather and Climate Extremes 29 (2020) 100267

Contents lists available at ScienceDirect

Weather and Climate Extremes

journal homepage: http://www.elsevier.com/locate/wace

Atmospheric circulation influence on temperature and precipitation individual and compound daily extreme events: Spatial variability and trends over southern South America

Matías Olmo [a,b,c,*], María Laura Bettolli [a,b,c], Matilde Rusticucci [a,b,c]

[a] Departamento de Ciencias de la Atmósfera y los Océanos, Facultad de Ciencias Exactas y Naturales, Universidad de Buenos Aires (DCAO-FCEN-UBA), 2do. piso, Pabellón II, Ciudad Universitaria, C1428EHA, Ciudad de Buenos Aires, Argentina
[b] Consejo Nacional de Investigaciones Científicas y Técnicas (CONICET), C1033AAJ, Av. Rivadavia, 1917, Buenos Aires, Argentina
[c] Instituto Franco Argentino Sobre Estudios de Clima y Sus Impactos (UMI-IFAECI), CNRS, UMI-IFAECI, CIMA, 2do. piso, Pabellón II, Ciudad Universitaria, C1428EGA, Buenos Aires, Argentina

ARTICLE INFO

Keywords:
Joint extremes
Precipitation
Temperature
Trends
Circulation types

ABSTRACT

Southern South America (SSA) is an extended region where temperature and precipitation daily extreme events have several impacts on the different socio-economic activities. In this work, their individual and compound occurrence over SSA and their association with atmospheric circulation were studied during 1979–2015, using meteorological stations and the CPC gridded dataset. Results were generally in good agreement between both datasets. The occurrence of a warm night (minimum temperature exceeding the 90th percentile) or a cold day (maximum temperature below the 10th percentile) significantly increases the probability of heavy precipitation (daily precipitation exceeding the 75th percentile) in southern Chile and southeastern South America. These compound events were regionally conditioned by specific circulation types. In addition, both individual and compound extremes showed trends in the different sub-regions. On one hand, heavy precipitation exhibited a significant increase over central-eastern Argentina and Uruguay, northeastern Argentina and southern Brazil during the warm season, and a significant decrease in central and southern Chile during the cold season. On the other hand, warm (cold) extremes generally presented significant upward (downward) trends. Compound events showed significant positive trends for selected regions, in some cases coincident with trends in individual extremes. Changes in the frequency of circulation patterns were found to partly influence some of these trends, like the increases in heavy precipitation and warm extremes during the warm season.

1. Introduction

Climate extremes that occur close together in space or time have lately become more recognised, since the combination of drivers and hazards contributes to societal or environmental risk. In this context, the Intergovernmental Panel on Climate Change (IPCC) defines a compound extreme event when two or more extreme events occur simultaneously or successively, when different extreme events combined imply an amplification of the impacts, or when individual events that are not extreme by themselves lead to an extreme event or impact when they occur together, inducing to an emerging risk (IPCC, 2012). Zscheischler et al. (2018) argue that a better understanding of compound events can improve projections of potential high impact events and can provide a better intercommunication between the different disciplines and decision makers.

Temperature and precipitation compound events have been widely analysed in different scales and regions around the world (Tencer et al., 2014; Orth et al., 2016; Hao et al., 2018a). However, the investigation on compound extremes, their changes and impacts in southern South America (SSA) (approximately 22–57°S, 50–70°W) has received only limited attention so far. SSA is one of the most populated regions of South America, where large cities such as Buenos Aires, Rosario and Santiago de Chile are located. The region is exposed to extreme events that strongly affect socio-economic activities, energy demand and health. Heavy precipitation events have responses of the landscape, surface water and aquifer systems, often leading to overflows and floods in many regions of SSA, causing several fatalities and great economic losses (Gatti et al., 2019; Esper Angillieri et al. 2017; Jordan et al.,

* Corresponding author. Departamento de Ciencias de la Atmósfera y los Océanos (DCAO-FCEN-UBA)
E-mail address: molmo@at.fcen.uba.ar (M. Olmo).

https://doi.org/10.1016/j.wace.2020.100267
Received 19 December 2019; Received in revised form 19 June 2020; Accepted 22 June 2020
Available online 26 June 2020
2212-0947/© 2020 The Authors. Published by Elsevier B.V. This is an open access article under the CC BY-NC-ND license (http://creativecommons.org/licenses/by-nc-nd/4.0/).

2015). Even more, Almeira et al., 2016 evidenced the effect of summer heatwaves in mortality in Buenos Aires and Rosario, particularly for elderly population. Hence, the combination of these extreme events may lead to larger and widespread impacts to human society and the environment than those from individual extremes alone (Hao et al., 2018b; IPCC, 2012). In this regard, previous works have evidenced the joint occurrence of extremes in some areas of SSA. Tencer et al. (2016) analysed daily extreme temperature and heavy precipitation compound events during the period 1961–2000 focused on La Plata Basin. The authors showed that, for the warm season, the probability of heavy precipitation significantly increases with warm nights occurring simultaneously, and with cold days on the next day of the heavy precipitation event. Based on monthly data of three reference meteorological stations over central Argentina, Barrucand et al. (2014) showed that warm and dry conditions were significantly more frequent than cool and dry conditions.

Several studies on individual extremes have shown changes in terms of their frequency and intensity during the recent period in SSA (Donat et al. 2013; Rusticucci, 2012; Skansi et al. 2013). Rusticucci et al. (2016) found, for the central region of Argentina, that trends of temperature extremes showed warming conditions, with a significant decrease in the frequency of cold nights and days and a significant increase in the warm days, though important intermonthly variability was detected. For heavy precipitation, Re and Barros (2009) and Penalba and Robledo (2010) found in southeastern South America predominantly positive trends during the second half of the 20th century, especially in the frequency and intensity of this event during austral summer and spring. Nevertheless, no studies have been done about temporal variability and trends in extreme temperature and heavy precipitation compound events in the recent period over SSA.

Classifications of atmospheric circulation are useful for studying past and recent climatic changes and comprehend the links between large-scale atmospheric processes and local weather (Cahynová and Huth, 2016). The occurrence of temperature and precipitation extremes over South America has been associated with diverse forcings in different temporal scales, such as sea surface temperature anomalies, teleconnection patterns, synoptic systems, and more (Cavalcanti, 2012; Rusticucci et al., 2016; Penalba et al., 2013, 2016). For describing atmospheric circulation, a typical procedure is the classification of circulation patterns (CPs). These classification schemes are practical tools for studying different aspects of climatic surface variables; in particular, the attribution of observed trends and future changes (Cahynová and Huth, 2016). Changes in atmospheric circulation are important for local climate change since they could lead to greater or smaller changes in climate in a particular region than elsewhere (IPCC, 2012). Analyses of attribution of climate change by CPs were done for other regions (Cahynová and Huth, 2009; Nilsen et al., 2014; Fleig et al., 2015) and assessed the fraction of climatic trends that can be attributed to a changing frequency of CPs. Notwithstanding, this approach has not been explored in SSA yet, and even less for extreme events.

In this context, the purpose of the present work is to evaluate both the individual and compound occurrence of daily extreme temperature and heavy precipitation events in SSA during the recent period, comparing their representation in two different observational datasets. The main objectives are to analyse the trends on individual and compound extreme events in different regions of SSA and to assess the influence of atmospheric circulation on the spatial distribution and temporal changes of these events.

2. Data and methodology

2.1. Observed surface data

We employed daily accumulated precipitation (Pr) and maximum and minimum temperature (Tx and Tn, respectively) observed at meteorological stations, during the period 1979–2015 in SSA (Fig. 1). Data were provided by the National Weather Services of Argentina, Brazil, Paraguay and Uruguay, and the Center for Climate and Resilience Research of Chile. 178 out of 225 meteorological stations that were originally available around SSA were selected with less than 5% of missing data in most of them. Only few meteorological stations with less than 20% of missing data were also used in southern Brazil to guarantee spatial coverage. A quality control was performed for each selected station with special focus on possible outliers in the time series (Penalba et al., 2004; Rusticucci and Barrucand, 2001). Also, given that SSA is an extended region of South America characterized by a wide variety of climates, a regionalization of meteorological stations was used in some analyses for the sake of conciseness. In particular, the methodology employed by Castellano and De Gaetano (2016), based on Ward's clustering method, was used to objectively explore the regional behavior in the occurrence of individual and compound extremes. Meteorological stations were grouped according to how regularly different pairs of stations presented an extreme event of the same nature (see Section 2.2 for definition of extreme event), and a distance matrix was constructed from similarity measures between each pair of stations. Finally, Ward's method of hierarchical clustering (Ward, 1963) was applied to this distance matrix and stations were grouped. This procedure was replicated for all the extremes studied in this work, yielding different numbers of regions (between 4 and 8). The final number of clusters was then defined considering, in addition, the regional characteristics and climates regimes of the region (Prohaska, 1976). These regions are presented in Fig. 1.

In order to perform climate studies of spatial and temporal variability of extremes, long records of high-quality and high-resolution observational datasets are necessary. Moreover, since the occurrence of compound extremes is rare, the study of their long-term changes

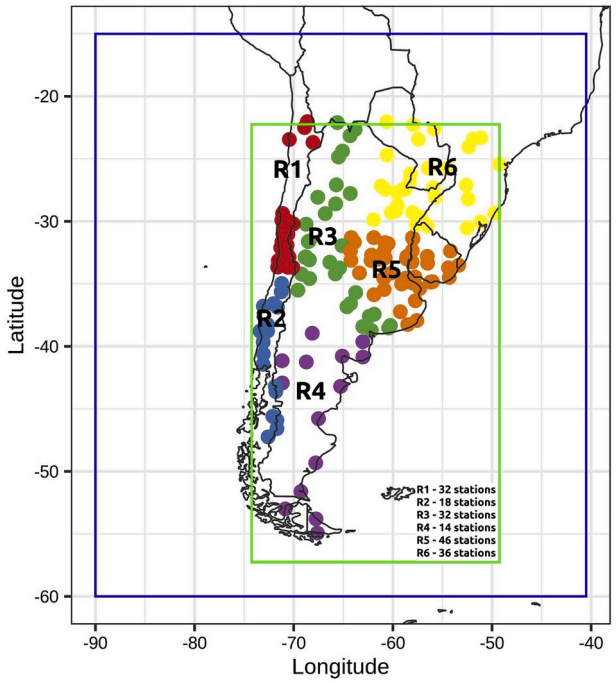

Fig. 1. Meteorological stations used in the study during the period 1979–2015. Colours and numbers indicate different climate regions: R1: northern Chile (arid and cold); R2: central and southern Chile (humid and cold); R3: arid diagonal region (dry); R4: Argentinian Patagonia (mainly dry and cold); R5: central-eastern SSA (humid and temperate); R6: northeastern Argentina and southern Brazil (humid and warm). CPC gridded precipitation and temperature were considered within the green box (land only), whereas ERA-Interim circulation was studied within the blue box. (For interpretation of the references to colour in this figure legend, the reader is referred to the Web version of this article.)

strongly depends on the existing data. In agreement, Hao et al. (2018b) concluded that efforts for understanding compound extremes should include observations with improved data availability, statistical model development and model simulations with improved representation of physical processes. However, in some areas of SSA, the density of meteorological stations may be low, and their temporal coverage may also be limited. Therefore, the study of the joint occurrence of extreme temperature and heavy precipitation should consider different perspectives and as much available information as possible. In line with this, the representation of daily individual and compound extremes was also evaluated in the daily gridded CPC Global dataset (CPC) from the NOAA Climate Prediction Center, with a resolution of 0.5°x0.5° (Xie et al., 2010), considering the same 3 variables.

2.2. Individual and compound extreme events definition

The IPCC has mentioned in its special report on "Managing the Risks of Extreme Events and Disasters to Advance Climate Change Adaptation" (IPCC, 2012) that compound events can be viewed as a special category of climate extremes, which are extreme either from a statistical perspective or associated with a specific threshold. In this work, percentile-based thresholds were used taking into account results from previous works over the region (Robledo et al., 2019; Tencer et al., 2014, 2016; Penalba and Robledo, 2010; Rusticucci et al., 2016) and the recommendations by Hao et al. (2018b) for studying the compound temperature and precipitation extremes. Following the methodology used in Tencer et al. (2016), daily heavy precipitation events (Pr75) were defined as those days when the accumulated precipitation exceeded the 75th percentile of the empirical distribution of rainy days ($Pr \geq 1$ mm). This percentile was based on a 29-days moving window centered on each calendar day. Similarly, warm days (nights) (Tx90, Tn90) corresponded to those days when Tx (Tn) exceeded the 90th percentile of the empirical distribution of all days, considering a 15-days moving window. Cold days (nights) (Tx10, Tn10), were recorded when Tx (Tn) was below the 10th percentile of its empirical distribution, with the same moving window. Then, a compound extreme event was defined as the joint occurrence of one of the mentioned temperature extremes and a Pr75 event. A 3-day window was considered for this definition, in order to bear in mind the different span of time for measurements of daily precipitation (12 UTC to 12 UTC of next day) and extreme daily temperatures (12 UTC and 0 UTC of the same local day).

The dependence between extremes was tested using a contingency table, by applying a 1-tailed chi-squared test at the 5% level of significance (Tencer et al., 2014; Wilks, 2011). The null hypothesis for this test is that the events are independent and, in consequence, the occurrence of Pr75 is not conditioned by a temperature extreme. Under this hypothesis, the expected joint probability can be calculated as the product of the two individual event probabilities and compared with the observed joint probability.

In order to visualize the strength of the relationship, the observed conditional probability of each compound extreme was presented as a ratio (Equation 1) over the expected probability of heavy precipitation in the absence of a relationship, that is the probability of Pr75 alone.

$$Ratio = \frac{P(Pr75 \mid Textreme)}{P(Pr75)} = \frac{P(Pr75 \mid Textreme)}{0.25{*}P(rainy\ days)}$$

Equation 1: Ratio between the observed conditional probability of each compound extreme event over the expected probability of heavy precipitation in the absence of a relationship.

In this way, ratios between 0 and 1 imply that the probability of the compound event is smaller than the probability of heavy precipitation alone, then the temperature extreme do not condition the precipitation event. On the other hand, ratios bigger than 1 mean that the occurrence of a temperature extreme increases the probability of heavy precipitation. The study was carried out separately for the austral warm (October to March) and cold (April to September) seasons. For each season, mean seasonal values of the percentiles used to define the extremes are presented in the supplementary material (Fig. S1).

2.3. Synoptic circulation

For the description of atmospheric circulation in SSA, daily CPs were generated by a obliquely rotated T-mode principal components analysis classification (PCA), which stands for its temporal and spatial stability, its ability to reproduce predefined dominant patterns, and little dependence on pre-set parameters (Stryhal and Huth, 2018; Huth, 2000). We considered daily geopotential height at the 500 hPa level (z500) from the ERA-Interim reanalysis of the European Center for Medium-Range Weather Forecasts (Dee et al., 2011). z500 fields form the columns in the input matrix **X**, whereas grid points form the rows. The method consists in expressing a data matrix as a product of two matrices $\mathbf{X} = \mathbf{Z}\ \mathbf{F'}$, where **Z** is the matrix of component scores and **F** the matrix of component loadings. Each component explains a fraction of the total variance and they are orthogonal (uncorrelated). The orthogonality constraint in synoptic patterns turns out to be unrealistic and therefore, oblique rotations relax this constraint to gain accuracy in the interpretation of the patterns. The oblimin rotation algorithm then computes the matrix of oblique rotation **Q** such that $\mathbf{F}\ \mathbf{Q} = \mathbf{S}$, where **S** is the new structure loading matrix which contains the correlation of the original variables **X** with the oblique factors. Finally, each daily z500 field is grouped with the pattern for which it has the highest structure loading. More details about this methodology can be found in Huth (2000) and Lattin et al. (2003). Circulation types were determined based on daily z500 fields over an extended domain (Fig. 1) for the warm and cold season separately, in the period 1979–2015. The criteria for choosing the number of patterns was to retain the first principal components accounting for 99% of the explained variance. Also, a "scree test" was employed to obtain the number of clusters looking for the elbow in the curve (Lattin et al., 2003). This classification resulted in 8 dominant CPs for each season of the year.

In order to analyse the association between joint extremes and CPs, the probabilities of compound events given a specific CP were compared to their climatological probabilities by performing a binomial test, at the 5% level of significance (Wilks, 2011) at each station point or grid point for CPC, under the null hypothesis that there is no difference between both probabilities against the alternative hypothesis that the probability of an extreme event conditioned to a specific CP was greater than the climatological probability of that event. Thus, the rejection of the null hypothesis indicates that the specific CP significantly enhances the occurrence of the extreme.

2.4. Trends and attribution of climatic change

Observed trends of extreme events frequency were estimated for every station and grid point in the complete period 1979–2015. Although a 37-years period may seem relatively short, it was the longest period when a fair balance between the spatial and temporal coverage was obtained. The non-parametric Mann-Kendall test was used to determine the presence of monotonic upward or downward trends (Libiseller and Grimvall, 2002). Linear regression was also employed for comparison purposes (Chambers, 1992). Both trends were statistically tested at the 5% level of significance.

In order to assess the proportion of long-term climate changes on extreme events directly linked to circulation changes, the method of circulation-induced or "hypothetical" linear trends was employed (Cahynová and Huth, 2009; Nilsen et al., 2014; Fleig et al., 2015). This method assumes that changes in CPs frequencies are the only factor causing the observed climatic trends. All days classified with the same CP are considered to lead to the same expected climatic value of a given variable for each month. In this case, the expected values were the monthly mean frequencies of the extreme events conditioned to each CP

(averaged over the whole period, e.g., all Januaries of 1979–2015). Daily circulation-induced time series were generated by assigning the respective conditional monthly mean to the days within each of the 12 months when the specific CP occurred. From these, the circulation-induced time series of seasonal frequencies were obtained and their linear trends were calculated. These "hypothetical" (circulation-related) trends were then compared to the observed changes by dividing them by the observed linear trend of the extreme event. The generated trend ratio would be around 1 if the extreme event trend was caused only by changes in CPs frequencies. To avoid dividing the circulation-related trends by small values associated with insignificant real changes, only meteorological stations with observed trends significant at the 5% level were considered. It should be mentioned that some of the trends may not be attributable to changing CPs frequencies only, and other causes such as the changing internal properties of the CPs, also known as within-type changes, may be responsible for the observed climatic trends (Cahynová and Huth, 2009), which represents a limitation of the method. A detailed description of this method can be found in Cahynová and Huth (2009, 2016).

3. Results

3.1. Compound extreme events

For the warm season, Fig. 2a shows the ratios between the observed probability of each compound extreme event over the expected probability in the absence of a relationship at station points (left panels) and at the CPC grid points (right panels), whereas Fig. 2b shows the corresponding seasonal average frequency (SAF) of compound extremes to get a full picture of the climatology of compound extremes in SSA. A positive relationship between warm nights and heavy precipitation (Pr75+Tn90) was observed over the whole SSA region, stronger and significant in southern Chile and northeastern Argentina (R2 and R5) (see Section 2.2 for methodology). This result implicates that the probability of having Pr75 highly increased due to the occurrence of Tn90, probably associated to instability conditions common in the warm season, that leads to the development of precipitating systems in regions where this compound event is more frequent (R2, R3, R5 and R6) (Fig. 2b). Warm days and heavy precipitation occurring together (Pr75+Tx90) only showed an increase in the probability of Pr75 given the extreme temperature in R5, however ratios and SAFs found were smaller than the ones observed for Pr75+Tn90. Ratios in the other regions were below 1, which means that Pr75 resulted inhibited when extreme maximum temperature occurred in these sectors. Cold nights generally inhibited the occurrence of Pr75, with only few stations in the coastal part of R4, where Pr75+Tn10 presented small ratios above 1. However, this event was the least frequent of all compound extremes studied over SSA, with SAFs lower than 2 events per season over most of the region (Fig. 2b). On the other hand, cold days and heavy precipitation (Pr75+Tx10) showed significant and positive relationships over all SSA, probably related to the passage of cold fronts. This compound extreme was the most frequent over SSA and, particularly, in R1 and R6, with SAFs up to 8 in the meteorological stations database. However, in some sectors like R4, where Pr75+Tx10 signal was high, frequencies found were low. This implicates that, despite occurring only few times, these events were highly influenced by the temperature extreme.

During the cold season, relationships between extremes exhibited similar patterns to the warm season (Fig. 3a and b). Notwithstanding,

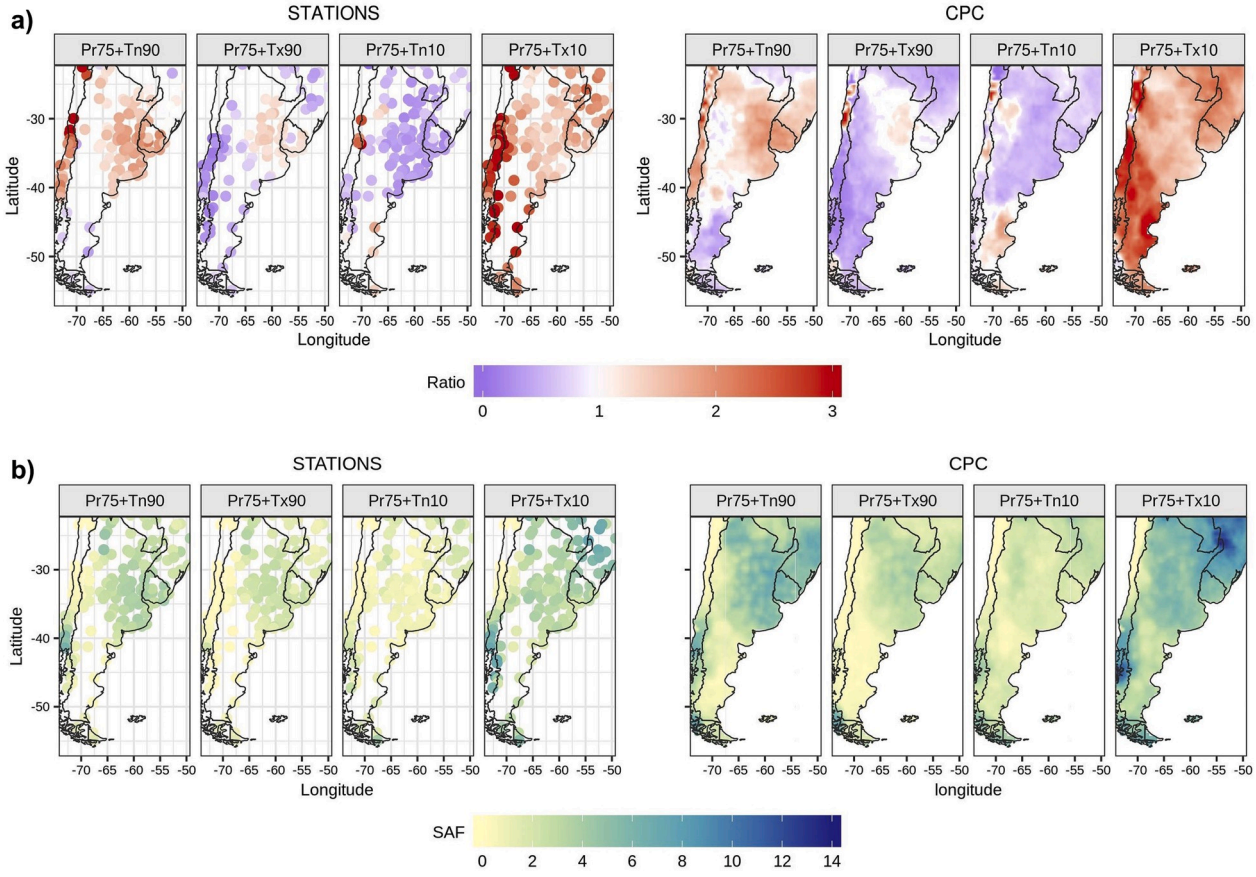

Fig. 2. a) Ratios between conditional and expected probabilities of extreme events over SSA for the warm season. On the left (right) panel, stations (CPC) results are shown. Filled symbols on stations indicate a significant relationship at the 5% level; b) seasonal average frequencies of each compound event (SAF) for the warm season (expressed as the average number of events).

Pr75+Tn90 ratios and frequencies resulted higher particularly in R4 and, in the case of Pr75+Tx10, R3 exhibited an increase in the relationship. On the contrary, a decrease in the ratios for this compound extreme was observed in R2 and R5, though frequencies were higher.

When analysing compound extremes as depicted by CPC, it was found that this dataset well reproduced the relationships between extremes, both in the magnitude and in the spatial distribution of ratios during the two seasons of the year (Figs. 2 and 3). However, it tended to overestimate the frequencies of compound events in both seasons. Indeed, CPC tended to overestimate both the probability and SAF of Pr75, particularly in R5 and R6 for the warm season (Fig. S2 in supplementary material). Since the probability of Pr75 is constructed as a product of 0.25 and the probability of rainy days, the observed overestimation of compound extremes frequency could be mainly due to the overestimation of the frequency of rainy days.

From the above analysis, it was evident that the most relevant compound events in SSA were Pr75+Tn90 and Pr75+Tx10, in both seasons. Even more, by analysing the joint occurrence of these compound extremes (not shown), it was found that they often happened together, depending on the region and season of the year. In more than 45% of Pr75+Tn90 events detected in southern Chile (R2) during the warm season, also a Pr75+Tx10 event occur, probably associated with instability and warm conditions previous to the passage of a system, that then decreased the temperature during the day, leading to a Pr75+Tx10 event. For Argentinian Patagonia (R4) and southeastern South America (R5 and R6), this percentage was around 20–30% during the warm season, and about 15% during the cold season. For these reasons, the following analyses will not address the other compound extremes.

3.2. Seasonal trends of individual and compound extreme events

Trends in compound extremes frequency can be dominated by one of the individual extremes involved. Even more, since the former ones result sub-samples of the individual events, it is important to also evaluate their temporal changes. For this reason, trends in individual and compound events in each station and grid point were analysed (see Figs. S3a and S3b for individual events). In order to summarize the results, areal average time series were considered as representative of each region (Figs. 4 and 5).

For the warm season, Pr75 showed positive and significant trends in R5 and R6, stronger in this last one, contrasting with the rest of SSA, where lower and non-significant changes were observed (Fig. 4a). In the CPC database, despite its trends presented the same sign as the meteorological stations, no region showed significance in its changes, and tended to overestimate Pr75 seasonal frequencies, particularly in R5 and R6. Tn90 exhibited significant upward trends in all the regions for the stations (Fig. 4a), except for R1, which showed a non-significant decrease. CPC generally underestimated Tn90 trends, and only showed significant changes in R3. For Tx90, significant positive trends were found over all SSA, in all the regions for both datasets, except for R1 where significant trends were only found in the meteorological stations. On the opposite, decreases for Tn10 and Tx10 were generally found: R3 showed significant negative trends for Tn10 in the stations, whereas R3, R5 and R6 presented significant decreases in Tx10 for both datasets. In addition, CPC underestimated the significant decrease in R1 detected in the stations data.

In the case of compound events, regional average series of regions with higher SAF were presented in Figs. 4b and 5b. During the warm season (Fig. 4b), significant upward trends in compound extremes were found in the stations of R3 and R6. Pr75+Tn90 trend was in agreement

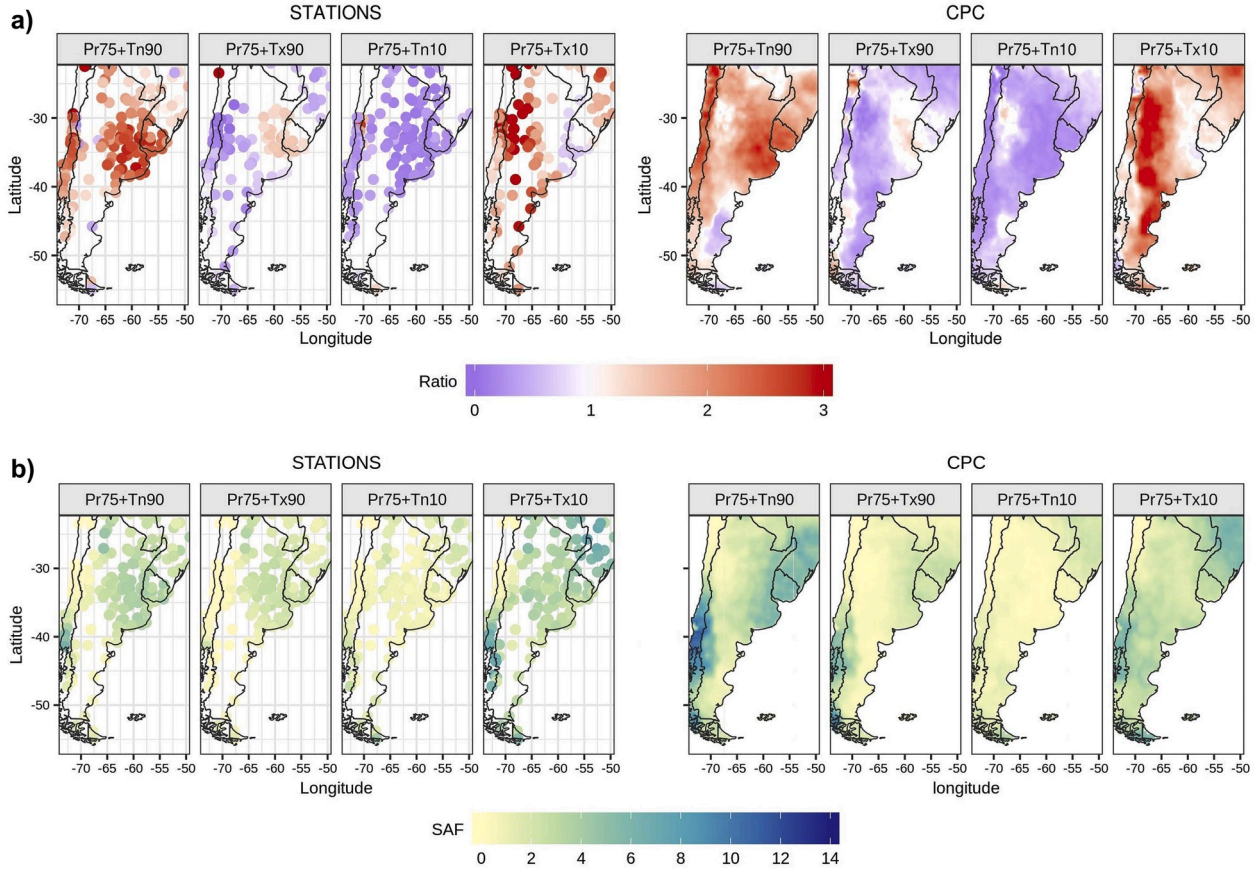

Fig. 3. Same as Fig. 2, but for the cold season.

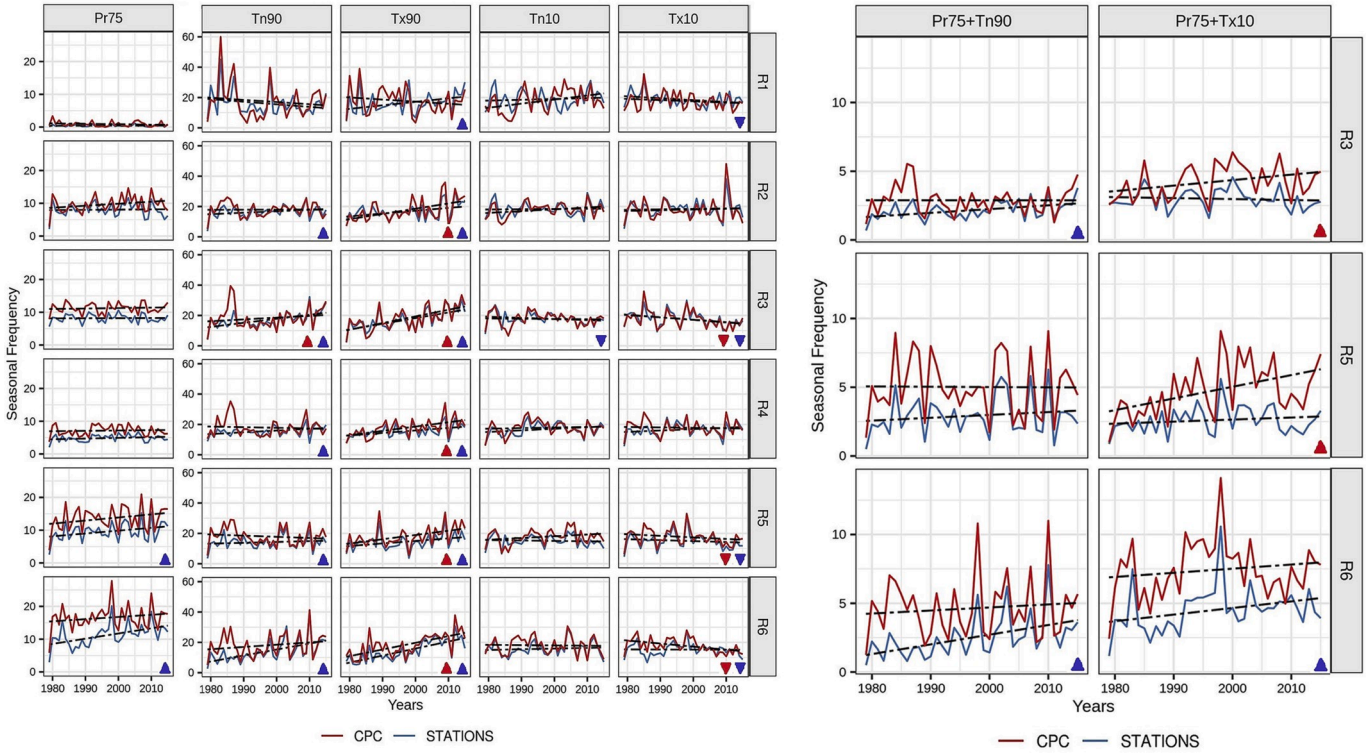

Fig. 4. Regional average temporal series of seasonal frequencies of individual and compound extreme events (a) and b), respectively) by sub-regions for the warm season. Upward and downward triangles indicate significant trends over each dataset. Linear trends are also included.

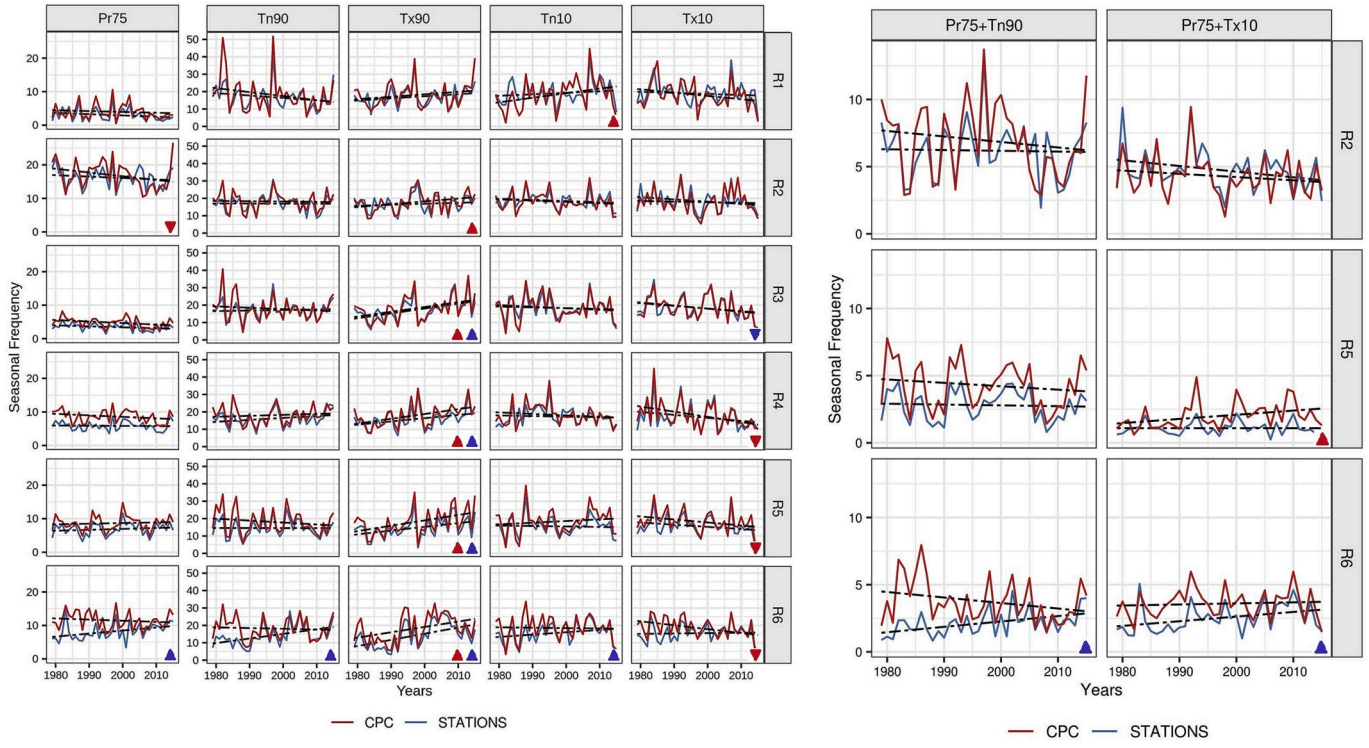

Fig. 5. Same as Fig. 4, but for the cold season.
(a) two-column fitting image (b) single-column fitting image.

with the trends in the individual events, whereas Pr75+Tx10 trend did not coincide with the trend in individual extremes, suggesting that the increases found in the compound event were mainly dominated by the upward trend in Pr75 over Tx10 negative trend (Fig. 4a). In R5 instead, where individual events trends showed a similar behavior that in R6, no significant trends were detected for compound events in the meteorological stations. In this region, Pr75+Tx10 only showed a positive trend in CPC. In R3, a positive trend was found for Pr75+Tn90 in agreement

with the upward trend in Tn90 for the stations. Pr75+Tx10 presented increases in CPC, but with no correspondence with individual events. As observed for Pr75 events, this dataset tended to overestimate the seasonal frequencies of compound extremes.

The increase in Pr75 detected for R5 and R6 in the stations data was in agreement with results by other authors (Penalba and Robledo, 2010; Haylock et al. 2006; Re and Barros, 2009), who observed increases in daily extreme precipitation using different thresholds and seasons over the second half of the 20th century. Particularly, the portions of SSA where Pr75 was more frequent and showed the greatest trends is affected by the South American low level jet (Rasmussen and Houze, 2016).

For temperature, results found in the present work showed generalized increases in warming conditions over almost all SSA. It was found that the number of regions with significant changes in temperature extremes was higher for warm extremes than for cold ones. This is in agreement with results by other authors for specific regions in SSA. Burger et al. (2018) pointed out significant warming trends during this season in part of R1, more noticeably in Tx, mainly for inland stations. Over central Argentina (portions of R3, R5 and R6), Rusticucci et al. (2016) also documented warming conditions, especially in October and November, though with high inter-monthly differences. When evaluating the relationship with atmospheric circulation, the authors pointed out that the intensification of the western part of the Atlantic anticyclone, which fosters warm air advection from the north, agreed with a greater frequency of warm extremes and with a lower frequency of cold extremes. Not only the positive trends in individual extremes, but also the upward trend in Pr75+Tn90 were in accordance with Kunkel (2003), who discussed that more events of heavy precipitation are expected with global warming, since water vapor availability for the precipitation systems tend to increase in a warmer atmosphere through the Clausius-Clapeyron equation, which describes the water holding capacity in the atmosphere. Even more, given that temperatures are expected to increase near the surface and decrease in the upper troposphere, thermodynamic instability needed for deep convection is also favored (Re and Barros, 2009). However, the temperature scaling of precipitation extremes is influenced by the different scales, the role of specific humidity, precipitation efficiency and regional weather patterns, which highlights the complexity of studying changes in intense rainfall events (Du et al., 2019; Drobinski et al., 2018; Barbero et al. 2017).

During the cold season (Fig. 5a), the stations detected significant and positive trends in Pr75 for R6. In the rest of SSA, results were not significant for the stations. In R2, both datasets exhibited a decrease in Pr75, but the trend detected by CPC was much stronger than in the stations data and was statistically significant. Trends for Tn90 were smaller than during the warm season, and only R6 presented significant positive changes for the stations data. In the case of Tx90, trends were similar to the warm season, with positive and significant changes in both datasets in most of SSA (R3 to R6). In southern Chile (R2), only CPC presented significance in the positive trend. For Tn10, results were more variable among the regions and between both datasets, while for Tx10, downward trends were found all over SSA in the two datasets, though CPC overestimated them in most of the regions. Significance was found for Tx10 in the stations only in R3, whereas CPC showed stronger and significant changes in R4 to R6.

For compound events during this season, decreases in Pr75+Tn90 were found in R2 and R5, while R6 exhibited significant positive trends in the stations (Fig. 5b). CPC overestimated the seasonal frequencies in all the regions and did not present significant changes in any of them. For Pr75+Tx10, a significant upward trend was found for R6 in the meteorological stations. CPC overestimated the frequencies in all regions and indicated significant positive changes for R5. As discussed in Section 3.1, the CPC overestimation of the probability of rainy days could be responsible of higher frequencies of Pr75 and, in consequence, a larger number of compound extremes compared to the stations.

Results for the cold season were congruent with previous studies. In particular, the decline observed for Pr75 in R2 is consistent with Quintana and Aceituno (2012), who found a downward trend in annual precipitation in the southern portion of central Chile, highly controlled by large-scale factors, resulting from a reduction in both the frequency of wet days and the intensity of precipitation. In addition, the increase detected in Tx90 for Argentinian Patagonia (R4) during this season was in accordance with Rusticucci and Barrucand (2004), who found similar results during the second half of the 20th century.

3.3. Relations with synoptic circulation

In order to analyse the synoptic circulation associated with individual and compound extremes, the relationship between CPs and the occurrence of each extreme event was studied for the warm and cold season separately. To this end, different circulation classifications of all days within each season of the year were performed. Fig. 6a shows the composites of daily anomalies of 500 hPa geopotential height for each CP during the warm season (CPw), whereas Figs. 6b and S4a (see Supplementary Material) show the percentage of days in each CPw when a compound and individual extreme event occurs, respectively. Figs. 7 and S4b show the respective results for the cold season. Circulation types exhibited positive and negative structures or centers that disturb the typical westerly flow of mid-latitudes at this level of the atmosphere. During the cold season, the centers' anomalies were more intense and located further north than in the warm season, in agreement with the seasonal behavior of the systems. This is the main reason to perform circulation classifications separately for the two seasons. Moreover, even though the number of CPs found was the same for each season, some of them had different configurations and therefore their regional effects on surface extremes were also different.

It was found that some CPs significantly enhanced the regional occurrence of individual and compound extremes (see Section 2.3 for methodology). CP1w was linked with both compound events in southern Chile (R2) in more than 12% of the days when this pattern was present (Fig. 6b). The associated circulation exhibited a strong center of negative anomalies in the southern Pacific Ocean favoring the occurrence of these extremes. This pattern presented some similarities with CP7w, which also favored both events in R2, though with a more weakened negative center in the Pacific Ocean. Under the influence of CP6w, in around 10% of the days a Pr75+Tn90 event was happening in southern Chile and central-northeastern Argentina (R2, R5 and R6). For Pr75+Tx10, this percentage was similar. In these regions, CP6w, which represents a short-wave disturbance dominating SSA, significantly increased the probability of having Pr75 occurring together with Tn90 or Tx10. The configuration of anomalies over the Pacific Ocean favored the intrusion of cold and humid air from the south-west that locates the extreme events little further north in R2 (when comparing with the effect of CP1w and CP7w). Whereas the dipolar structure of negative anomalies extended to the southern sector of SSA and positive anomalies over the Atlantic Ocean, allowed more humid and warm air from lower latitudes to enter the region stimulating instability conditions over R5 and R6. This was in accordance with the low-level circulation characterized by Rasmussen and Houze (2016), that enhances intense precipitation events over those areas. In the case of CP8w, a wide negative center was found in the Atlantic Ocean, which entered the continent and was related with Pr75+Tx10 in R5 and R6 and with Pr75+Tn90 in the last region. CP4w and CP5w (the less frequent patterns of the warm season) were related to Pr75+Tx10, particularly in R6 for the first one and more widespread east of the Andes for the last one. Both patterns showed a dipolar structure of anomalies which favored the cold air intrusion from the southeast in the former and south in the latter, locating the extremes in different regions.

When analysing the effects on individual extremes (Fig. S4a), different CPs took leading roles. For instance, CP4w and CP5w favored Tx10 east of the Andes while CP6w and CP8w favored these events in

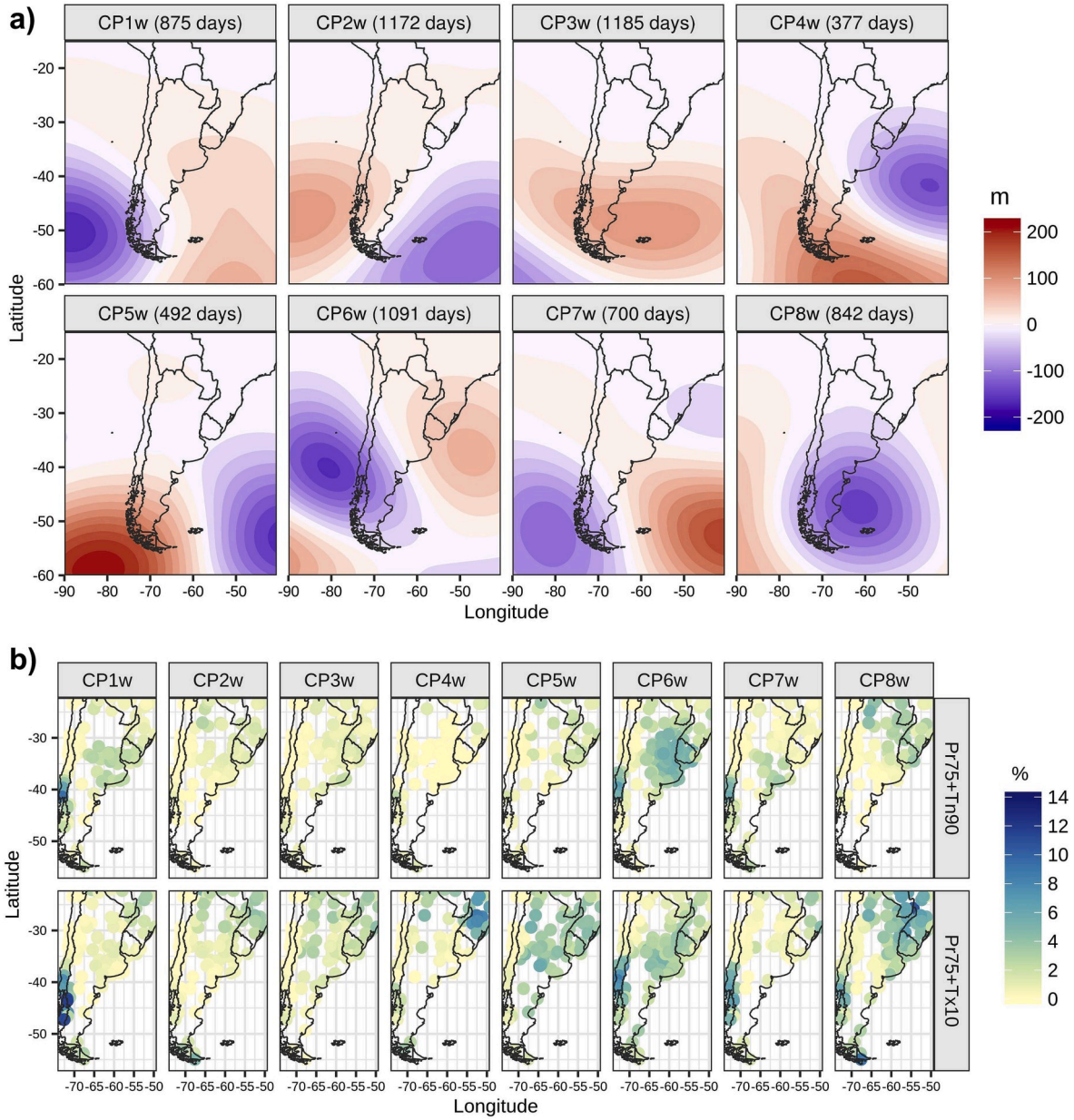

Fig. 6. a) composites of 500 hPa geopotential height anomalies for each daily circulation pattern for the warm season (CPw) (in meters); b) percentage of days in each CPw when a compound extreme event occurs. Only stations with statistically significant results were plotted.

Southern Chile and Southern Argentina (R2 and R4). Tx10 in R1 and R3 (northern Chile and northwestern Argentina) was linked to CP3w occurrence. CP1w favored the occurrence of Tn90 over almost the whole region analysed, while CP3w and CP6w had influence over the southern (R2 and R4) and northern (R3, R5 and R6) regions respectively. As it was expected, the effects of the CPs on Pr75 were more restricted to local regions and similar to joint extremes as the sample size is reduced to these events (Fig. S4a).

For the cold season, effects of the CPs on compound events were less widespread than in the warm season and conditioned to some specific CPs (Fig. 7). CP1c exhibited a similar structure than CP1w, with a center of negative anomalies in the southern Pacific Ocean associated to the occurrence of both compound extremes in R2. CP2c showed congruent results with CP4w in the extremes frequencies, favoring Pr75+Tx10 in southern Brazil (R6) due to the configuration of anomalies that lead to the intrusion of cold air masses to lower latitudes, typical of this season of the year. In the case of CP3c, which was similar to CP6w pattern but with stronger anomalies located further north, Pr75+Tn90 and Pr75+Tx10 were enhanced along Chile (R2 and the southern portion of R1). Unlike the warm season, this pattern only favored Pr75+Tn90 in central Argentina (R5) and was also related with Pr75+Tx10 over R4, being the only pattern associated with compound extremes over this region. When analysing individual extremes (see Fig. S3b in Supplementary Material), it was clear the effect of CP2c on cold extremes over the whole region of Southern South America, but as described earlier, its influence on joint extremes was confined to southern Brazil. CP4c and CP6c also contributed with cold temperatures but in R3, R5 and R6, whereas CP3c and CP1c contributed with warm extremes over these regions (Fig. S4b).

It is of interest to highlight that the relationship between CPs and extreme events (both individual and compound) was also analysed for CPC, finding similar results to the station points (not shown).

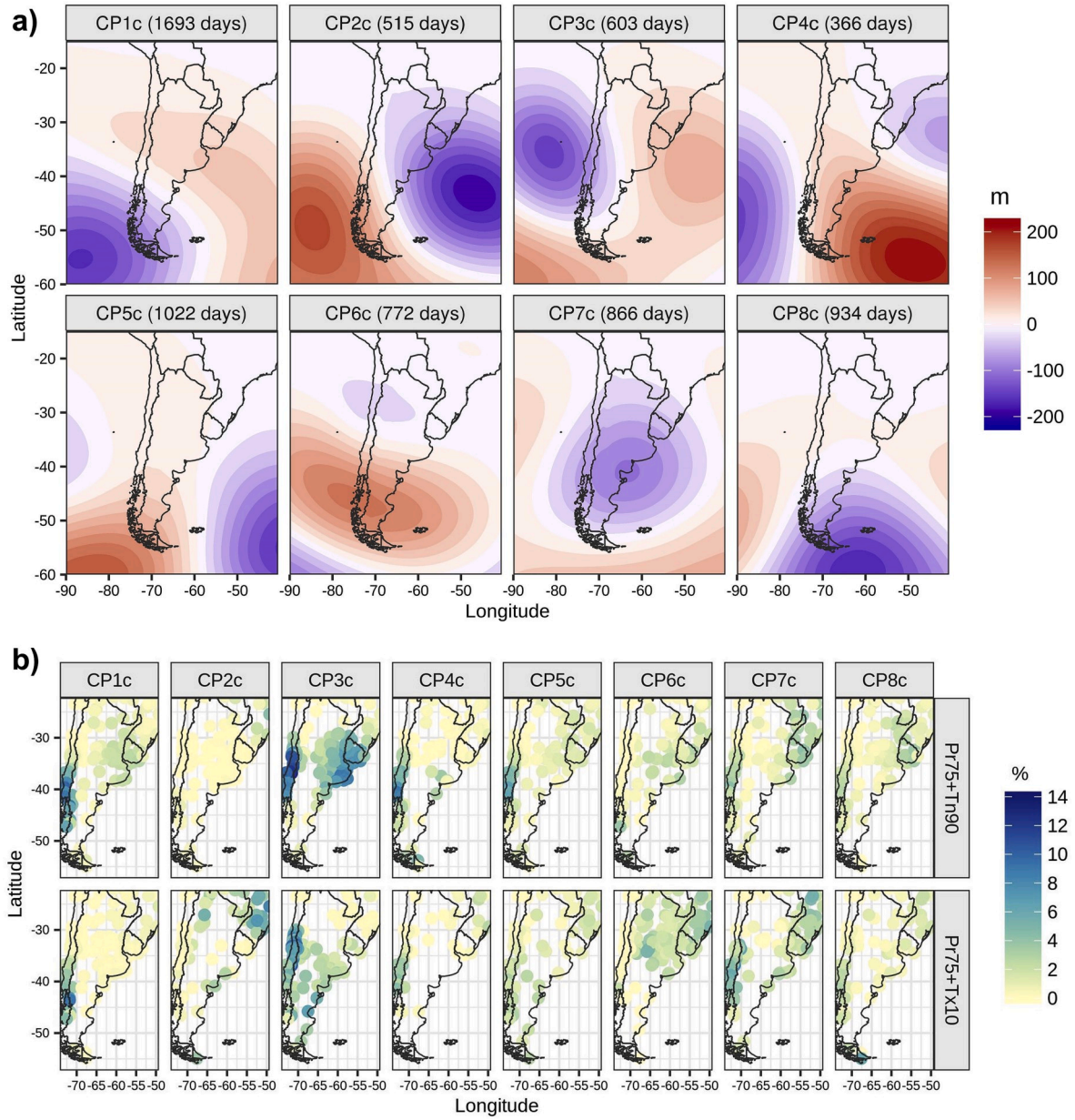

Fig. 7. Same as Fig. 6, but for the cold season.

3.4. Attribution of trends in extreme events

Efforts to associate precipitation and temperature variability with tropospheric circulation over southern South America have been the focus of different studies from different perspectives (Saurral et al., 2016; Maenza et al., 2017; Quintana and Aceituno, 2012; Barrucand et al., 2008). Understanding the physical mechanisms behind their trends continues to be one of the biggest challenges, particularly when it comes to extremes. Among few studies addressing this topic, Robledo et al. (2019) found that trends in the intensity of daily heavy precipitation (Pr75 intensity) in central-eastern Argentina could be related to the combined influence of both multidecadal variability and trends of tropical ocean SST anomalies. Rusticucci et al. (2016) found that the intensification of the western part of the Atlantic anticyclone, inducing warm and humid air advection from the north, agreed with greater frequencies of warm extremes (Tn90 and Tx90) and with lower frequencies of cold extremes (Tn10 and Tx10).

Results found in the previous section showed that individual and compound extremes are regionally related to flow anomalies at middle levels of the atmosphere. Therefore, it is of interest to evaluate to what extent the detected temporal changes in frequency of extremes may be attributed to changes in circulation. To this end, linear trends of CPs seasonal frequencies were estimated (Table 1). Some patterns presented significant trends, positive for CP3w and negative for CP1w and CP3c, whereas other CPs showed slight changes (though non-significant), such as the increase in CP6w. Thus, the decrease in CP3c frequency may be associated with the downward frequency of compound events in R2.

Table 1
Linear trends of CPs seasonal frequencies expressed as days per 37 years (period of study). Bold values indicate significant changes.

CP1w	CP2w	CP3w	CP4w	CP5w	CP6w	CP7w	CP8w
−7	−1	**6**	−2	0	4	3	−3
CP1c	CP2c	CP3c	CP4c	CP5c	CP6c	CP7c	CP8c
3	1	**−5**	2	−3	2	0	0

While upward frequencies in compound extremes in R5 and R6 may be related to the increases in CP6w, which favors warm and humid flow from the north in agreement with the results from Rusticucci et al. (2016) for individual extremes.

In order to explore if these changes in CPs frequencies, considering the combinations of all CPs in each season, influences the occurrence of individual and compound extremes, ratios between circulation-related - "hypothetical" - and observed seasonal trends were calculated (see Section 2.4 for methodology). This analysis was performed for both stations and CPC data, with no noticeable differences between them. For brevity, the analysis is only shown for the stations data in the boxplots presented in Figs. 8 and 9, separately for each sub-region in the two seasons of the year. Only stations with observed linear trends significant at the 5% level of confidence were chosen for the comparison. Additionally, for compound events, emphasis was made in those regions with high seasonal average frequencies and where the observed trends were stronger and significant (Fig. 9).

During the warm season, Pr75 trends were explained by circulation changes in about 50% in R5, whereas trend ratios for the other regions exhibited values around 25% or less (Fig. 8a). In relation to temperature events, warm extremes showed mostly positive trend ratios, while cold extremes presented lower values, close to zero. For Tn90, mean values of trend ratios were always positive, about 20–30% in R3, R5 and R6, though in R5, high variability among meteorological stations was detected. In Chile, these ratios presented less spatial variability and an average value of 20%. In the case of Tx90, trend ratios were more regionally homogenous than in Tn90, mostly positive and up to 75%. For Tn10 and Tx10, no clear links between circulation changes and trends were found, since trend ratios were regularly distributed around zero. During the cold season (Fig. 8b), this method generally failed to interpret the observed changes for Pr75 and Tn90. In the case of Tx90, increases in R1 and R4 could be associated with CPs changing frequency in an average value of 20% and 30%, respectively. For Tn10, significant trends in R6 (Fig. S3) may be attributed to circulation changes in about 20%, whereas Tx10 trends in R2 and R4 were partially explained by changes in CPs frequency.

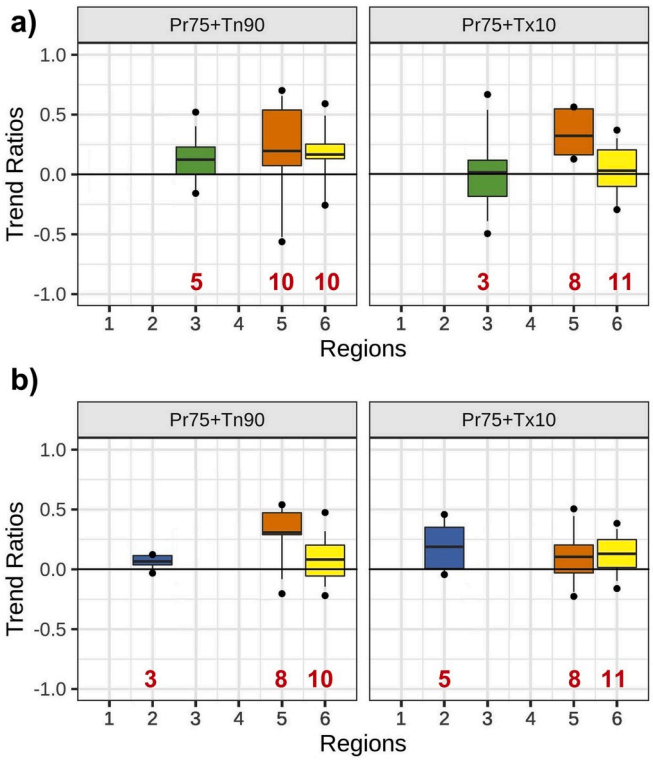

Fig. 9. Boxplots of the ratios between "hypothetical" (circulation-related) and observed seasonal trends of selected compound extremes at meteorological stations in the regions of interest for: a) warm season; b) cold season. Only values with significant observed trends at the 5% level were considered.

When attributing trends in compound extremes for the stations data to CPs changes, more clear signals were observed for Pr75+Tn90 and Pr75+Tx10 in R5, though there was important variability within

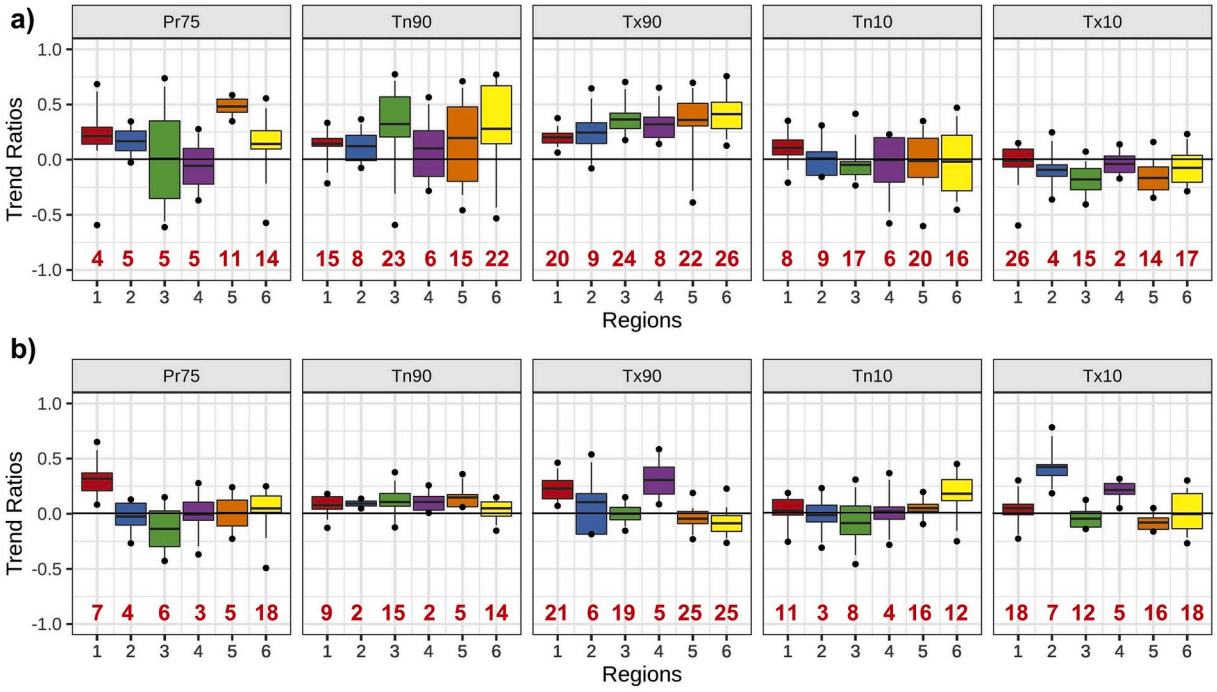

Fig. 8. Boxplots of the ratios between "hypothetical" (circulation-related) and observed seasonal trends of individual extremes at meteorological stations by sub-regions (1–6) for: a) warm season; b) cold season. Only stations with significant trends at the 5% level were considered (the number of stations considered in each region is shown in red). (For interpretation of the references to colour in this figure legend, the reader is referred to the Web version of this article.)

stations (Fig. 9). No clear influence on climatic trends was found for R3, where trend ratios were around zero for Pr75+Tn90 and even negative for Pr75+Tx10, indicating that their changes may not be only related with large-scale circulation and may be caused by some other local factors too (Cahynová and Huth, 2016). In the cold season, changes in joint extremes for R5 and R6 were related to circulation changes, with trend ratios that averaged between 15% and 25% (Fig. 9b), whereas maximum values reached 50%. R2, characterized by a decrease in compound extremes according to the stations data (Fig. 5b), showed ratios around 25% and up to 50% for Pr75+Tx10, while values for Pr75+Tn90 were close to zero.

4. Discussion and conclusions

Southern South America (SSA) is a wide region with different climates, exposed and sensitive to extreme events. Even more, these events occurring together can magnify the effects of them alone. Therefore, their characterization and study constitute the basis not only for understanding their possible evolution in a changing climate but also for determining the exposure and vulnerability of societies and social-ecological systems.

This work shows that some regions of SSA region are the scene not only of individual precipitation and temperature extremes but also of daily precipitation and temperature extremes occurring together. Pr75 associated mostly with Tn90 and Tx10 were found to be the most frequent compound events, particularly in southern Chile and northeastern SSA (Figs. 2 and 3). Temporal changes were detected for both individual and compound extremes over different regions of SSA. Pr75 presented positive trends in central-eastern Argentina and northeastern SSA, significant for the first one in the warm season and for the last one during both seasons (Figs. 4a and 5a). A decrease was observed for southern Chile during the cold season as well, but only in the CPC dataset. In addition, warming conditions were mainly observed, with significant increases in Tn90 and Tx90 and significant decreases in Tn10 and Tx10 in both seasons. Overall, Tx showed more homogeneous trends that Tn over SSA. Previous studies have found generally larger rates of warming from Tn than from Tx (Donat et al. 2013; Skansi et al. 2013). However, this discrepancy could be due to the sensibility of trends to the period of study and to the season used for constructing the indices. Compound events exhibited significant upward trends for some regions (Figs. 4b and 5b): Pr75+Tn90 in the arid diagonal region during the warm season and in northeastern SSA during both seasons, whereas Pr75+Tx10 showed significant increases in the arid diagonal region and northeastern Argentina for the warm season according to CPC and in northeastern SSA for the stations data during both seasons. Additionally, in agreement with the decline observed in Pr75, decreases in compound events were detected in southern Chile during the cold season, though those trends were not significant.

This study also highlights the importance of considering different sources of information when addressing the study of extreme temperature and precipitation in a daily basis, in order to obtain a comprehensive spatial-temporal characterization and to account for observational uncertainty as well. This is particularly valuable for regions like SSA, where data availability is often sparse and, therefore, continuous assessments integrating new data are needed. In this work, the CPC gridded dataset was used together with station data to characterize individual and compound extremes. CPC is one of the few observational gridded datasets available at a daily scale for SSA including all the three variables of interest (precipitation, minimum and maximum temperature). These aspects, together with its usefulness for climate model evaluation, make it easier to handle and more attractive than station data. In general terms, CPC was in agreement with station data as for the spatial and temporal characterization of individual and joint extremes. CPC often overestimated extremes frequencies, which may be related to a larger number of rainy days in this dataset, and presented some differences on the long-term temporal variability (trends) with the station data. This appeared to be greater in northern Chile, maybe due to the lack of spatial coverage of stations in that region. Due to these discrepancies between datasets, the use of different sources of information is recommended when evaluating climate extremes in the region.

Understanding the link between atmospheric circulation and precipitation and temperature at different time scales over SSA has been the subject of different studies (Saurral et al., 2016; Maenza et al., 2017; Quintana and Aceituno, 2012). This is an even more challenging task when it comes to climate extremes, and when their temporal changes are of particular interest (Robledo et al., 2019; Rusticucci et al., 2016). In this sense, the present study is a contribution to better understand the circulation associated with the spatial-temporal variability of different climatic extremes in SSA. It was shown that the occurrence of individual and compound extremes was regionally conditioned by specific circulation patterns (Figs. 6 and 7). A dipolar structure of negative geopotential height anomalies at 500 hPa over the Pacific Ocean and positive anomalies over the Atlantic Ocean favored the intrusion of cold and humid air from the south-west contributing to Pr75+Tn90 and Pr75+Tx10 in southern Chile, while enhanced the occurrence of these compound extremes over central-eastern Argentina and northeastern SSA associated with more humid and warm air from lower latitudes. In the cold season, the leading structure that enhanced compound extremes presented a similar configuration of anomalies than the one mentioned for the warm season, but with flow anomalies more intense and located further north.

The attribution of trends suggested that the changing frequency of CPs could explain some of the temporal changes in extremes. During the warm season, for individual events, higher trend ratios were found for warm extremes in comparison with cold extremes. In this season, the influence was more explicit for Tx90, which presented mostly positive trend ratios, more regionally homogeneous than for Tn90. This indicates that changes in atmospheric circulation would be responsible for a large portion of the observed warm season warming, whereas no clear association could be found for trends in cold extremes. Pr75 upward trend in central-eastern Argentina and northeastern SSA was associated with circulation changes in about 25% and 50%, respectively. For compound events, despite more variability within regions, a stronger signal was found for central-eastern Argentina. During the cold season, only a small influence was found for Pr75+Tx10 in southeastern South America and southern Chile. This analysis contributes to the still incipient studies for the region on attribution of climatic trends to changes in circulation. However, results emerged from this approach may not be enough to robustly infer about to what extent changes in the frequency of atmospheric circulation patterns are responsible of changes in extremes frequencies. This may be due to the use of a single circulation classification; therefore, the use of more synoptic classifications is recommended for future studies (Cahynová and Huth, 2009).

Overall, this work exhibited that many regions of SSA are exposed to both individual and compound climate extremes, which were characterized by temporal changes in the recent period and were associated with specific synoptic circulation patterns. These results motivate further studies about compound extremes at different time scales that have not been addressed here, such as hot and dry summers occurring together, but that were subject of study in different regions of the world (Orth et al., 2016; Sedlmeier et al., 2018; Zscheischler et al., 2018). Moreover, different classifications of circulation patterns would help to better understand the spatial and temporal variability of compound extremes as well as different attribution methods would shed light on further details of the recent climate changes, and will be subject of future studies.

Declaration of competing interest

The authors declare that they have no known competing financial interests or personal relationships that could have appeared to influence the work reported in this paper.

Acknowledgements

This work was supported by the University of Buenos Aires 2018-20020170100117BA, 20020170100357BA and the ANPCyT PICT-2018-02496 projects. The CPC Global Temperature and Global Unified Precipitation data was provided by the NOAA/OAR/ESRL PSD, Boulder, Colorado, USA, from their Web site at https://www.esrl.noaa.gov/psd/.

Appendix A. Supplementary data

Supplementary data to this article can be found online at https://doi.org/10.1016/j.wace.2020.100267.

References

Almeira, G., Rusticucci, M., Suaya, M., 2016. Relación entre mortalidad y temperaturas extremas en Buenos Aires y Rosario. Meteorológica 41, 65–79.

Barbero, R., Westra, S., Lenderink, G., Fowler, H.J., 2017. Temperature-extreme precipitation scaling: a two-way causality? Int. J. Climatol. 38, e1274–e1279. https://doi.org/10.1002/joc.5370.

Barrucand, M., Rusticucci, M., Vargas, W., 2008. Temperature extremes in the south of South America in relation to Atlantic Ocean surface temperature and Southern Hemisphere circulation. J. Geophys. Res. 113, D20111. https://doi.org/10.1029/2007JD009026.

Barrucand, M., Vargas, W., Bettolli, M.L., 2014. Warm and cold dry months and associated circulation in the humid and semi-humid Argentine region. Meteorol. Atmos. Phys. 123, 143–154.

Burger, F., Brock, B., Montecinos, A., 2018. Seasonal and elevational contrasts in temperature trends in Central Chile between 1979 and 2015. Global Planet. Change 162, 136–147.

Cahynová, M., Huth, R., 2009. Changes of atmospheric circulation in central Europe and their influence on climatic trends in the Czech Republic. Theor. Appl. Climatol. 96, 57–68.

Cahynová, M., Huth, R., 2016. Atmospheric circulation influence on climatic trends in Europe: an analysis of circulation type classifications from the COST733 catalogue. Int. J. Climatol. 36, 2743–2760.

Castellano, C.M., De Gaetano, A., 2016. A multi-step approach for downscaling daily precipitation extremes from historical analogues. Int. J. Climatol. 36, 1797–1807.

Cavalcanti, I., 2012. Large scale and synoptic features associated with extreme precipitation over South America: a review and case studies for the first decade of the 21st century. Atmos. Res. 118, 27–40.

Chambers, J.M., 1992. Linear models. In: Chambers, J.M., Hastie, T.J. (Eds.), Chapter 4 of Statistical Models. Wadsworth & Brooks/Cole.

Dee, D.P., Uppala, S.M., Simmons, A.J., Berrisford, P., Poli, P., Kobayashi, S., Andrae, U., Balmaseda, M.A., Balsamo, G., Bauer, P., Bechtold, P., Beljaars, A.C.M., van de Berg, L., Bidlot, J., Bormann, N., Delsol, C., Dragani, R., Fuentes, M., Geer, A.J., Haimberger, L., Healy, S.B., Hersbach, H., Hólm, E.V., Isaksen, L., Kållberg, P., Köhler, M., Matricardi, M., McNally, A.P., Monge-Sanz, B.M., Morcrette, J.J., Park, B.K., Peubey, C., de Rosnay, P., Tavolato, C., Thépaut, J.N., Vitart, F., 2011. The ERA-Interim reanalysis: configuration and performance of the data assimilation system. Q. J. Roy. Meteorol. Soc. 137, 553–597. https://doi.org/10.1002/qj.828.

Donat, M.G., co-authors, 2013. Updated analyses of temperature and precipitation extreme indices since the beginning of the twentieth century: the HadEX2 dataset. J. Geophys. Res.: Atmosphere 118, 2098–2118.

Drobinski, P., Silva, N.D., Panthou, G., et al., 2018. Scaling precipitation extremes with temperature in the Mediterranean: past climate assessment and projection in anthropogenic scenarios. Clim. Dynam. 51, 1237–1257. https://doi.org/10.1007/s00382-016-3083-x.

Du, H., Alexander, L.V., Donat, M.G., Lippmann, T., Srivastava, A., Salinger, J., et al., 2019. Precipitation from persistent extremes is increasing in most regions and globally. Geophys. Res. Lett. 46, 6041–6049. https://doi.org/10.1029/2019GL081898.

Esper Angillieri, M.Y., Perucca, L., Vargas, N., 2017. Catastrophic flash flood triggered by an extreme rainfall event in El Rodeo village, January 2014. Northwestern Pampean Ranges of Argentina. Geogr. Ann. Phys. Geogr. 99 (1), 72–84.

IPCC Managing the Risks of Extreme Events and Disasters to Advance Climate Change Adaptation (eds Field, C. B. et al.), 2012. Cambridge Univ. Press.

Fleig, A.K., Tallaksen, L.M., James, P., Hisdal, H., Stahl, K., 2015. Attribution of European precipitation and temperature trends to changes in synoptic circulation. Hydrol. Earth Syst. Sci. 19, 3093–3107.

Gatti, I., Robledo, F., Hurtado, S., Canneva, J., Moreira, D., Re, M., Briche, E., Falco, M., Kazimierski, L., Micou, A.P., 2019. Anticipating the Flood. Community-based cartography for disaster flood events in Argentina. Proceedings of the International Cartographic Association 2.

Hao, Z., Hao, F., Singh, V.P., Zhang, X., 2018a. Changes in the severity of compound drought and hot extremes over global land areas. Environ. Res. Lett. 13, 124022.

Hao, Z., Singh, V.P., Hao, F., 2018b. Compound extremes in hydroclimatology: a review. Water 10, 718.

Haylock, M.R., Peterson, T.C., Alves, L.M., Ambrizzi, T., Anunciacao, Y.M.T., Baez, J., Barros, V.R., Berlato, M.A., Bidegain, M., Coronel, G., Corradi, V., Garcia, V.J., Grimm, A.M., Karoly, D., Marengo, J.A., Marino, M.B., Moncunill, D.F., Nechet, D., Quintana, J., Rebello, E., Rusticucci, M., Santos, J.L., Trebejo, I., Vincent, L., 2006. Trends in Total and Extreme South American Rainfall in 1960 2000 and Links with Sea Surface Temperature. Journal of Climate 19, 1490–1512. https://doi.org/10.1175/JCLI3695.1.

Huth, R., 2000. A circulation classification scheme applicable in GCM studies. Theor. Appl. Climatol. 67, 1–18.

Jordan, T., Riquelme, R., González, G., co-authors, 2015. Hydrological and Geomorphological Consequences of the Extreme Precipitation Event of 24–26 March 2015, Chile. Congreso Geológico Chileno, La Serena. October 2015.

Kunkel, K., 2003. North American trends in extreme precipitation. Nat. Hazards 29, 291–305.

Lattin, J.M., Douglas Carroll, J., Green, P.E., 2003. Analyzing Multivariate Data. Thomson Brooks/Cole.

Libiseller, C., Grimvall, A., 2002. Performance of partial Mann-Kendall tests for trend detection in the presence of covariates. Environmetrics 13, 71–84. https://doi.org/10.1002/env.507.

Maenza, R., Agosta Scarel, E.A., Bettolli, M.L., 2017. Climate change and precipitation variability over the western "Pampas" in Argentina. Int. J. Climatol. 37, 445–463.

Nilsen, I., Fleig, A.K., Tallaksen, L.M., Hisdal, H., 2014. Recent Trends in Monthly Temperature and Precipitation Patterns in Europe. Hydrology in a Changing World: Environmental and Human Dimensions, vol. 363. IAHS Publ.

Orth, R., Zscheischler, J., Seneviratne, S.I., 2016. Record dry summer in 2015 challenges precipitation projections in central Europe. Sci. Rep. 6, 28334.

Penalba, O.C., Robledo, F., 2010. Spatial and temporal variability of the frequency of extreme daily rainfall regime in the La Plata Basin during the 20th century. Climatic Change 98 (Issue 3), 531–550.

Penalba, O.C., Rivera, J.A., Pantano, V.C., 2004. The CLARIS LPB database: constructing a long-term daily hydro-meteorological dataset for La Plata Basin, Southern South America. Geoscience Data Journal 1, 20–29.

Penalba, O.C., Bettolli, M.L., Krieger, P.A., 2013. Surface circulation types and daily maximum and minimum temperatures in southern La Plata basin. J. of Applied Meteorology and Climatology 52, 2450–2459.

Penalba, O.C., Rivera, J.A., Pántano, V.C., Bettolli, M.L., 2016. Extreme rainfall, hydric conditions and associated atmospheric circulation in the southern La Plata Basin. Clim. Res. 68, 215–229.

Prohaska, F., 1976. The climate of Argentina, Paraguay and Uruguay. World Surv. Climatol. 12, 13–73.

Quintana, J.M., Aceituno, P., 2012. Changes in the rainfall regime along the extratropical west coast of South America (Chile): 30-43°S. Atmósfera 25 (1), 1–12.

Rasmussen, K.L., Houze Jr., R.A., 2016. Convective initiation near the Andes in subtropical South America. Mon. Weather Rev. 144, 2351–2374.

Re, M., Barros, V., 2009. Extreme rainfalls in SE south America. Climatic Change 96, 119.

Robledo, F., Vera, C., Penalba, O., 2019. Multi-scale features of the co-variability between global sea surface temperature anomalies and daily extreme rainfall in Argentina. Int. J. Climatol. 119–136. https://doi.org/10.1007/s10584-009-9619-x.

Rusticucci, M., 2012. Observed and simulated variability of extreme temperature events over South America. Atmos. Res. 106, 1–17.

Rusticucci, M., Barrucand, M., 2001. Climatología de temperaturas extremas en la Argentina. Consistencia de datos. Relación entre la temperatura media estacional y la ocurrencia de días extremos. Meteorológica 26, 69–83.

Rusticucci, M., Barrucand, M., 2004. Observed trends and changes in temperature extremes over Argentina. J. Clim. 17 (No. 20), 4099–4107.

Rusticucci, M., Barrucand, M., Collazo, S., 2016. Temperature extremes in the Argentina central region and their monthly relationship with the mean circulation and ENSO phases. Int. J. Climatol. 37 (6), 3003–3017.

Saurral, R.I., Camilloni, I.A., Barros, V.R., 2016. Low-frequency variability and trends in centennial precipitation stations in southern South America. Int. J. Climatol. 37 (Issue 4), 1774–1793.

Sedlmeier, K., Feldmann, H., Schädler, G., 2018. Compound summer temperature and precipitation extremes over central Europe. Theor. Appl. Climatol. 131, 1493–1501.

Skansi, M., co-authors, 2013. Warming and wetting signals emerging from analysis of 363 changes in climate extreme indices over South America. Global Planet. Change 100, 295–307.

Stryhal, J., Huth, R., 2018. Classifications of winter atmospheric circulation patterns: validation of CMIP5 GCMs over Europe and the North Atlantic. Clim. Dynam. 52 (5-6), 3575–3598.

Tencer, B., Weaver, A., Zwiers, F., 2014. Joint occurrence of daily temperature and precipitation extreme events over Canada. J. of Applied Meteorology and Climatology 53, 2148, 2162.

Tencer, B., Bettolli, M.L., Rusticucci, M., 2016. Compound temperature and precipitation extreme events in Southern South America: associated atmospheric circulation and simulations by a multi-RCM ensemble. Clim. Res. 68, 183–199.

Ward, J.H., 1963. Hierarchical grouping to optimize an objective function. J. Am. Stat. Assoc. 58, 236–244. https://doi.org/10.1080/01621459.1963.10500845.

Wilks, D.F., 2011. Statistical Methods in the Atmospheric Sciences, third ed. Ac. Press, p. 627pp.

Xie, P., Chen, M., Shi, W., 2010. CPC global gauge-based analysis of daily precipitation, Preprints. In: 24th Conf. On Hydrology, vol. 2. Amer. Meteor. Soc, Atlanta, GA.

Zscheischler, J., Westra, S., Van Den Hurk, B.J.J.M., Seneviratne, S.I., Ward, P.J., et al., 2018. Future climate risk from compound events. Nat. Clim. Change 8 (6), 469–477.